

Electronic Supplementary Information

A π -Extended Triphenylamine Based dopant-free Hole-Transporting Material for Perovskite Solar Cells *via* Heteroatom Substitution

Mengyao Hao^a, *Davin Tan*^b, *Weijie Chi*^{,b,c*}, *Zesheng Li*^{a*}

^a Key Laboratory of Cluster Science of Ministry of Education, Beijing Key Laboratory of Photoelectronic/Electrophotonic Conversion Materials, School of Chemistry and Chemical Engineering, Beijing Institute of Technology, Beijing 100081, China

^b Fluorescence Research Group, Singapore University of Technology and Design, 8 Somapah Road, 487372 Singapore

^c Department of Chemistry, School of Science, Hainan University, Haikou, 570228, China.

Corresponding authors

E-mail: weijie_chi@hainanu.edu.cn

E-mail: zeshengli@bit.edu.cn

Contents

Computational details.....	1
Tables	
Table S1 Calculated transition energy E_{0-0} (eV), maximum wavelengths λ_{ab} (nm), oscillator strength f of absorption, Transition (HOMO→LUMO) and the contribution of heteroatoms to the hole for the first excited state, transition energy E_1 (eV), maximum wavelengths λ_{em} (nm) of emission and Stokes shifts (nm).....	3
Table S2 Specific data for crystal structure analysis, including Space group, Cell volume (cm ³), Density (g/cm ³), Total energy (eV), Van der Waals energy (eV), Length a (Å), b (Å), c (Å).....	4
Table S3 The transfer integrals V_{DA} (eV), hole-hopping rate k_h (s ⁻¹), centroid-to-centroid distances r (cm), the hole mobility μ_h (cm ² v ⁻¹ s ⁻¹) for main hopping pathways selected and the total hole mobility μ (cm ² v ⁻¹ s ⁻¹) based on the predicted crystalline structures of OMeTPA-TPA	5
Table S4 The transfer integrals V_{DA} (eV), hole-hopping rate k_h (s ⁻¹), centroid-to-centroid distances r (cm), the hole mobility μ_h (cm ² v ⁻¹ s ⁻¹) for main hopping pathways selected and the total hole mobility μ (cm ² v ⁻¹ s ⁻¹) based on the predicted crystalline structures of OMeTPA-B	6
Table S5 The transfer integrals V_{DA} (eV), hole-hopping rate k_h (s ⁻¹), centroid-to-centroid distances r (cm), the hole mobility μ_h (cm ² v ⁻¹ s ⁻¹) for main hopping pathways selected and the total hole mobility μ (cm ² v ⁻¹ s ⁻¹) based on the predicted crystalline structures of OMeTPA-C	7
Table S6 The transfer integrals V_{DA} (eV), hole-hopping rate k_h (s ⁻¹), centroid-to-centroid distances r (cm), the hole mobility μ_h (cm ² v ⁻¹ s ⁻¹) for main hopping pathways selected and the total hole mobility μ (cm ² v ⁻¹ s ⁻¹) based on the predicted crystalline structures of OMeTPA-Si	8
Table S7 The transfer integrals V_{DA} (eV), hole-hopping rate k_h (s ⁻¹), centroid-to-centroid distances r (cm), the hole mobility μ_h (cm ² v ⁻¹ s ⁻¹) for main hopping pathways selected and the total hole mobility μ (cm ² v ⁻¹ s ⁻¹) based on the predicted crystalline structures of OMeTPA-	

Ge	9
Table S8 The transfer integrals V_{DA} (eV), hole-hopping rate k_h (s^{-1}), centroid-to-centroid distances r (cm), the hole mobility μ_h ($cm^2 v^{-1} s^{-1}$) for main hopping pathways selected and the total hole mobility μ ($cm^2 v^{-1} s^{-1}$) based on the predicted crystalline structures of OMeTPA-N	10
Table S9 The transfer integrals V_{DA} (eV), hole-hopping rate k_h (s^{-1}), centroid-to-centroid distances r (cm), the hole mobility μ_h ($cm^2 v^{-1} s^{-1}$) for main hopping pathways selected and the total hole mobility μ ($cm^2 v^{-1} s^{-1}$) based on the predicted crystalline structures of OMeTPA-P	11
Table S10 The transfer integrals V_{DA} (eV), hole-hopping rate k_h (s^{-1}), centroid-to-centroid distances r (cm), the hole mobility μ_h ($cm^2 v^{-1} s^{-1}$) for main hopping pathways selected and the total hole mobility μ ($cm^2 v^{-1} s^{-1}$) based on the predicted crystalline structures of OMeTPA-As	12
Table S11 The transfer integrals V_{DA} (eV), hole-hopping rate k_h (s^{-1}), centroid-to-centroid distances r (cm), the hole mobility μ_h ($cm^2 v^{-1} s^{-1}$) for main hopping pathways selected and the total hole mobility μ ($cm^2 v^{-1} s^{-1}$) based on the predicted crystalline structures of OMeTPA-O	13
Table S12 The transfer integrals V_{DA} (eV), hole-hopping rate k_h (s^{-1}), centroid-to-centroid distances r (cm), the hole mobility μ_h ($cm^2 v^{-1} s^{-1}$) for main hopping pathways selected and the total hole mobility μ ($cm^2 v^{-1} s^{-1}$) based on the predicted crystalline structures of OMeTPA-S	14
Table S13 The transfer integrals V_{DA} (eV), hole-hopping rate k_h (s^{-1}), centroid-to-centroid distances r (cm), the hole mobility μ_h ($cm^2 v^{-1} s^{-1}$) for main hopping pathways selected and the total hole mobility μ ($cm^2 v^{-1} s^{-1}$) based on the predicted crystalline structures of OMeTPA-Se	15
Table S14 The combination modes and surface adsorption energy (eV) of central core and perovskite surface (001 face).	16
Table S15 The optimized structures of Pb-N and Pb-X models of central core and perovskite surface (001 face).	17

Table S16 The Pb-N (Pb-X) bond lengths (\AA) of the most stable combination mode of central core and perovskite surface (Corresponding to the structure in Figure S5). 18

Figures

Figure S1 The chemical structures and full names of the study molecules..... 19

Figure S2 Molecular electrostatic potentials (*ESP*) of **R-TPA** and **R-X**, along with the Max positive *ESP*, Max negative *ESP*, and the difference between positive and negative *ESP* of the investigated molecules, the unit is kcal mol^{-1} 20

Figure S3 Calculated absorption spectra of the study molecules. 21

Figure S4 The main neighboring hole-hopping pathways selected based on the predicted crystal structures for all molecules, along with The reorganization energy k_h (s^{-1} , green one), centroid-to-centroid distances r (cm, blue one), transfer integrals V (eV, orange one) and the hole mobility μ_h ($\text{cm}^2 \text{v}^{-1} \text{s}^{-1}$, purple one) for main hopping pathways selected based on the predicted crystalline structures. 22

Figure S5 The combination mode of central core and perovskite surface (001 face)..... 23

Figure S6 The most stable combination mode of central core and perovskite surface (001 face) 24

Figure S7 The distance of perovskite/**R-TPA** and perovskite/**R-Se** systems..... 25

Figure S8 The distribution of partial atomic charges for **R-B**, **R-C**, **R-Si**, **R-Ge**, **R-N**, **R-P**, **R-As**, **R-O**, and **R-S**, where blue represents negative charge and pink represents positive charge..... 26

References..... 27

Computational details

Hole transport properties for isolated molecules

The hole mobility of the investigated molecules is calculated by using the Einstein relation:¹

$$\mu = \frac{er^2}{2k_B T} k \quad (\text{S1})$$

where e is the charge. r denotes the distance between two mass centers.

The Marcus theory with the hopping model is employed to describe the hole transport behavior.

The charge hopping rate (k) is expressed as:²

$$k = \frac{4\pi^2}{h} v^2 \frac{1}{\sqrt{4\pi k_B T}} \exp\left[-\frac{\lambda}{4k_B T}\right] \quad (\text{S2})$$

where k_B represents the Boltzmann constant, T is the temperature in Kelvin, and h denotes the Planck constant. λ represents the reorganization energy, which is calculated by using the adiabatic potential energy surface method. In this work, only internal reorganization energy is considered. The reorganization energy can be expressed as follows:³

$$\lambda = (E_0^* - E_0) + (E_+^* - E_+) \quad (\text{S3})$$

where E_0^* and E_+^* are the total energies of neutral and cationic molecules with the geometries of the cationic and neutral species, respectively. E_+ and E_0 are the total energies of the cationic and neutral molecules in their lowest energy geometries, respectively.

v denotes the transfer integral, which is obtained by adopting a direct approach at the M06-2X/6-31G (d, p) level. In our work, v can be written as:⁴

$$v = \langle \psi_i^{\text{HOMO}} | F | \psi_f^{\text{HOMO}} \rangle \quad (\text{S4})$$

where ψ_i^{HOMO} and ψ_f^{HOMO} represent the HOMOs of the isolated molecules 1 and 2. F is the Fock operator for the dimer, which can be calculated as: $F = SC\varepsilon C^{-1}$

The Kohn-Sham Orbital C and eigenvalue ε are evaluated by diagonalizing the zeroth-order Fock matrix. S denotes the overlap matrix for the dimer.

CH₃NH₃PbI₃/HTMs interfacial properties

The plane wave energy cutoff is set to 500 eV with the application of periodic boundary conditions for the structures of HTM molecule and CH₃NH₃PbI₃ (797 atoms), and all atomic positions are fully relaxed during optimization (residual forces, <0.01 eV/Å). The k-point grids of $1 \times 1 \times 1$ and $2 \times 2 \times 1$ are adopted for geometry optimization and electronic properties

calculations, respectively. Van der Waals (vdW) interactions are considered with Grimme's DFT-D3 correction to describe weak interactions between the HTM molecule and $\text{CH}_3\text{NH}_3\text{PbI}_3$.⁵

Table S1 Calculated transition energy E_{0-0} (eV), maximum wavelengths λ_{ab} (nm), oscillator strength f of absorption, Transition (HOMO \rightarrow LUMO) and the contribution of heteroatoms to the hole for the first excited state, transition energy E_1 (eV), maximum wavelengths λ_{em} (nm) of emission and Stokes shifts (nm).

Molecule	E_{0-0} (eV)	λ_{ab} (nm)	f	Transition (HOMO \rightarrow LUMO)	hole- contribution (eV)	E_1 (eV)	λ_{em} (nm)	Stokes shifts
OMeTPA-TPA	3.21	386	1.6554	78%	/	2.66	467	80
OMeTPA-B	2.45	507	0.0591	9%	5.09	2.15	576	70
OMeTPA-C	3.19	388	1.359	87%	0.36	2.67	464	76
OMeTPA-Si	3.05	407	1.5223	89%	0.95	2.47	503	96
OMeTPA-Ge	3.22	385	1.7473	74%	0.49	2.42	513	128
OMeTPA-N	2.45	506	0.3476	91%	18.83	1.78	695	190
OMeTPA-P	2.97	418	1.3491	89%	2.56	2.43	510	92
OMeTPA-As	2.96	419	1.3504	90%	1.82	2.40	516	96
OMeTPA-O	2.88	430	0.7733	88%	10.96	2.24	554	123
OMeTPA-S	2.61	476	0.6162	87%	17.45	2.16	573	97
OMeTPA-Se	2.50	496	0.5407	85%	19.63	2.04	607	112

Table S2 Specific data for crystal structure analysis, including Space group, Cell volume (cm³), Density (g/cm³), Total energy (eV), Van der Waals energy (eV), Length a (Å), b (Å), c (Å).

Molecule	Space group	Cell volume	Density	Total energy	Van der Waals energy	Length a	Length b	Length c
OMeTPA-TPA	P21	3.64×10 ³	1.05	182.54	81.29	22.44	11.06	16.68
OMeTPA-B	P21	3.54×10 ³	1.11	260.25	95.43	17.49	27.52	7.40
OMeTPA-C	P21	3.46×10 ³	1.14	106.28	96.96	17.77	11.94	17.40
OMeTPA-Si	P-1	3.77×10 ³	1.09	140.89	105.29	11.40	20.36	17.15
OMeTPA-Ge	P21	3.83×10 ³	1.19	260.58	92.41	16.19	25.68	9.23
OMeTPA-N	P21	3.31×10 ³	1.20	-18.37	93.50	18.13	12.15	16.20
OMeTPA-P	P21	3.60×10 ³	1.15	233.76	106.10	15.92	20.26	11.54
OMeTPA-As	P21	4.33×10 ³	1.06	-1.08×10 ⁴	1.39×10 ³	25.83	6.98	27.06
OMeTPA-O	P21	3.45×10 ³	1.15	137.38	89.98	7.41	26.73	20.09
OMeTPA-S	P21	3.51×10 ³	1.18	154.46	93.17	8.15	22.10	24.63
OMeTPA-Se	P21	3.25×10 ³	1.42	-1.79×10 ⁴	2.38×10 ³	19.25	7.21	24.60

Table S3 The transfer integrals V_{DA} (eV), hole-hopping rate k_h (s^{-1}), centroid-to-centroid distances r (cm), the hole mobility μ_h ($cm^2 v^{-1} s^{-1}$) for main hopping pathways selected and the total hole mobility μ ($cm^2 v^{-1} s^{-1}$) based on the predicted crystalline structures of **OMeTPA-TPA**.

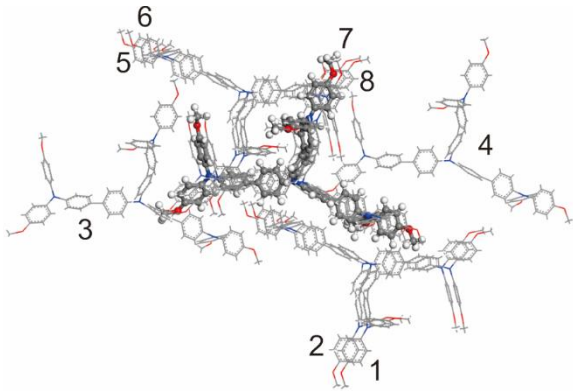
OMeTPA-TPA					
					
pathway	V_{DA}	k_h	r	μ_h	μ
1	9.0×10^{-5}	1.33×10^8	1.11×10^{-7}	3.13×10^{-5}	2.42×10^{-3}
2	8.97×10^{-5}	1.32×10^8	1.11×10^{-7}	3.10×10^{-5}	
3	-3.48×10^{-4}	1.99×10^9	1.67×10^{-7}	1.06×10^{-3}	
4	-3.44×10^{-4}	1.95×10^9	1.67×10^{-7}	1.04×10^{-3}	
5	-1.45×10^{-3}	3.46×10^{10}	1.07×10^{-7}	7.63×10^{-3}	
6	-1.46×10^{-3}	3.48×10^{10}	1.07×10^{-7}	7.67×10^{-3}	
7	1.10×10^{-3}	1.97×10^{10}	1.44×10^{-7}	7.83×10^{-3}	
8	1.10×10^{-3}	1.98×10^{10}	1.44×10^{-7}	7.88×10^{-3}	

Table S4 The transfer integrals V_{DA} (eV), hole-hopping rate k_h (s^{-1}), centroid-to-centroid distances r (cm), the hole mobility μ_h ($cm^2 v^{-1} s^{-1}$) for main hopping pathways selected and the total hole mobility μ ($cm^2 v^{-1} s^{-1}$) based on the predicted crystalline structures of **OMeTPA-B**.

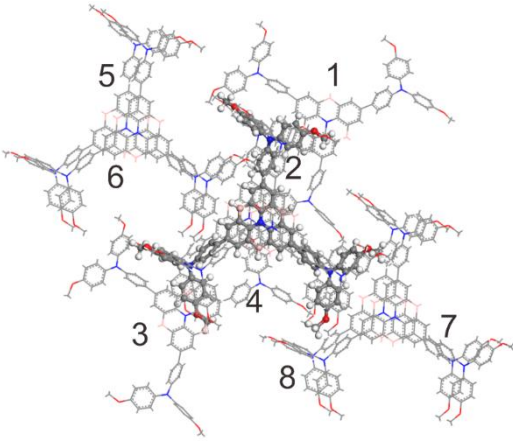
OMeTPA-B					
					
pathway	V_{DA}	k_h	r	μ_h	μ
1	1.03×10^{-3}	9.20×10^9	1.38×10^{-7}	3.39×10^{-3}	1.09×10^{-3}
2	-5.04×10^{-6}	2.21×10^5	7.41×10^{-8}	2.33×10^{-8}	
3	8.37×10^{-4}	6.09×10^9	1.38×10^{-7}	2.25×10^{-3}	
4	1.03×10^{-3}	9.20×10^9	1.38×10^{-7}	3.39×10^{-3}	
5	-2.16×10^{-4}	4.05×10^8	1.75×10^{-7}	2.38×10^{-4}	
6	-8.01×10^{-4}	5.58×10^9	1.98×10^{-7}	4.21×10^{-3}	
7	-7.97×10^{-4}	5.52×10^9	1.98×10^{-7}	4.17×10^{-3}	
8	-2.15×10^{-4}	4.02×10^8	1.75×10^{-7}	2.37×10^{-4}	

Table S5 The transfer integrals V_{DA} (eV), hole-hopping rate k_h (s^{-1}), centroid-to-centroid distances r (cm), the hole mobility μ_h ($cm^2 v^{-1} s^{-1}$) for main hopping pathways selected and the total hole mobility μ ($cm^2 v^{-1} s^{-1}$) based on the predicted crystalline structures of **OMeTPA-C**.

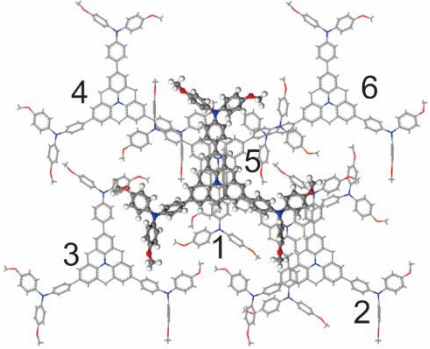
OMeTPA-C					
					
pathway	V_{DA}	k_h	r	μ_h	μ
1	-1.31×10^{-2}	2.21×10^{11}	4.17×10^{-8}	7.38×10^{-2}	2.89×10^{-2}
2	-6.29×10^{-3}	5.07×10^{11}	1.24×10^{-7}	1.49×10^{-1}	
3	-4.84×10^{-4}	3.00×10^9	1.86×10^{-7}	1.99×10^{-3}	
4	1.34×10^{-3}	2.30×10^{10}	1.96×10^{-7}	1.70×10^{-2}	
5	1.34×10^{-3}	2.30×10^{10}	1.95×10^{-7}	1.68×10^{-2}	
6	-4.85×10^{-4}	3.02×10^9	1.87×10^{-7}	2.03×10^{-3}	

Table S6 The transfer integrals V_{DA} (eV), hole-hopping rate k_h (s^{-1}), centroid-to-centroid distances r (cm), the hole mobility μ_h ($cm^2 v^{-1} s^{-1}$) for main hopping pathways selected and the total hole mobility μ ($cm^2 v^{-1} s^{-1}$) based on the predicted crystalline structures of **OMeTPA-Si**.

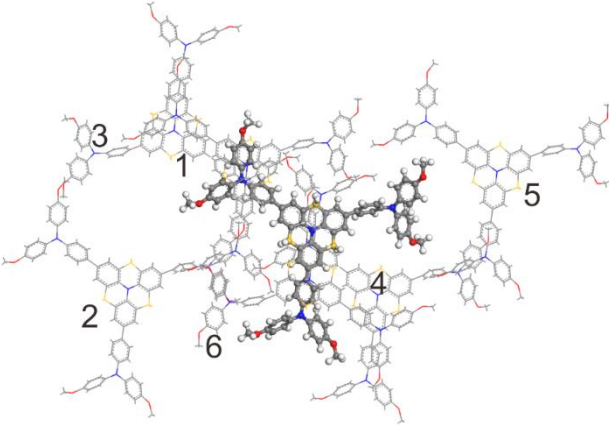
OMeTPA-Si					
					
pathway	V_{DA}	k_h	r	μ_h	μ
1	-5.79×10^{-3}	3.64×10^{11}	1.14×10^{-7}	9.09×10^{-2}	1.27×10^{-1}
2	-6.95×10^{-4}	5.25×10^9	2.23×10^{-7}	5.00×10^{-3}	
3	9.40×10^{-3}	9.59×10^{11}	2.02×10^{-7}	7.50×10^{-1}	
4	-5.78×10^{-3}	3.63×10^{11}	1.14×10^{-7}	9.08×10^{-2}	
5	-6.95×10^{-4}	5.25×10^9	2.23×10^{-7}	5.00×10^{-3}	
6	-6.11×10^{-3}	4.06×10^{11}	7.37×10^{-8}	4.23×10^{-2}	

Table S7 The transfer integrals V_{DA} (eV), hole-hopping rate k_h (s^{-1}), centroid-to-centroid distances r (cm), the hole mobility μ_h ($cm^2 v^{-1} s^{-1}$) for main hopping pathways selected and the total hole mobility μ ($cm^2 v^{-1} s^{-1}$) based on the predicted crystalline structures of **OMeTPA-Ge**.

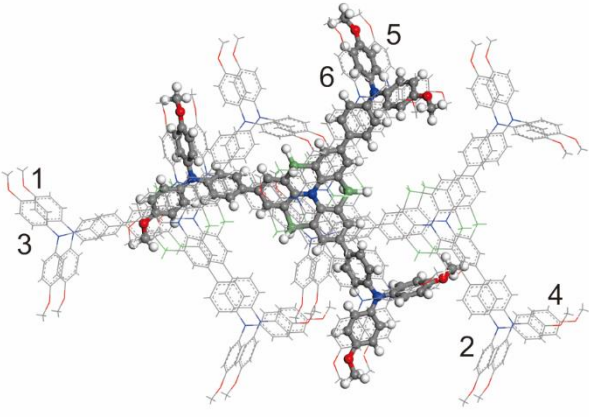
OMeTPA-Ge					
					
pathway	V_{DA}	k_h	r	μ_h	μ
1	-1.87×10^{-3}	1.76×10^{10}	2.08×10^{-7}	1.46×10^{-2}	3.90×10^{-3}
2	-2.21×10^{-4}	2.45×10^8	1.14×10^{-7}	6.13×10^{-5}	
3	-2.20×10^{-4}	2.44×10^8	1.14×10^{-7}	6.11×10^{-5}	
4	-1.87×10^{-3}	1.76×10^{10}	2.08×10^{-7}	1.46×10^{-2}	
5	-1.53×10^{-3}	1.17×10^{10}	1.22×10^{-7}	3.37×10^{-3}	
6	-1.53×10^{-3}	1.17×10^{10}	1.22×10^{-7}	3.38×10^{-3}	

Table S8 The transfer integrals V_{DA} (eV), hole-hopping rate k_h (s^{-1}), centroid-to-centroid distances r (cm), the hole mobility μ_h ($cm^2 v^{-1} s^{-1}$) for main hopping pathways selected and the total hole mobility μ ($cm^2 v^{-1} s^{-1}$) based on the predicted crystalline structures of **OMeTPA-N**.

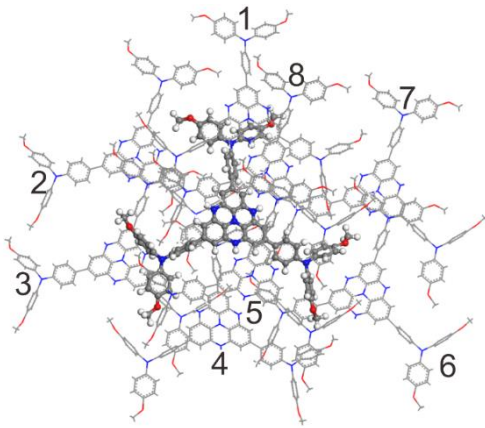
OMeTPA-N					
					
pathway	V_{DA}	k_h	r	μ_h	μ
1	-1.45×10^{-3}	9.81×10^8	1.22×10^{-7}	2.79×10^{-4}	9.221×10^{-5}
2	6.46×10^{-5}	1.96×10^6	1.43×10^{-7}	7.73×10^{-7}	
3	6.47×10^{-5}	1.96×10^6	1.43×10^{-7}	7.75×10^{-7}	
4	-1.448×10^{-3}	9.84×10^8	1.22×10^{-7}	2.79×10^{-4}	
5	-1.68×10^{-4}	1.32×10^7	8.59×10^{-8}	1.88×10^{-6}	
6	-2.50×10^{-5}	2.94×10^5	1.79×10^{-7}	1.81×10^{-7}	
7	6.92×10^{-5}	2.25×10^6	1.79×10^{-7}	1.38×10^{-6}	
8	-1.65×10^{-4}	1.28×10^7	8.59×10^{-8}	1.82×10^{-6}	

Table S9 The transfer integrals V_{DA} (eV), hole-hopping rate k_h (s^{-1}), centroid-to-centroid distances r (cm), the hole mobility μ_h ($cm^2 v^{-1} s^{-1}$) for main hopping pathways selected and the total hole mobility μ ($cm^2 v^{-1} s^{-1}$) based on the predicted crystalline structures of **OMeTPA-P**.

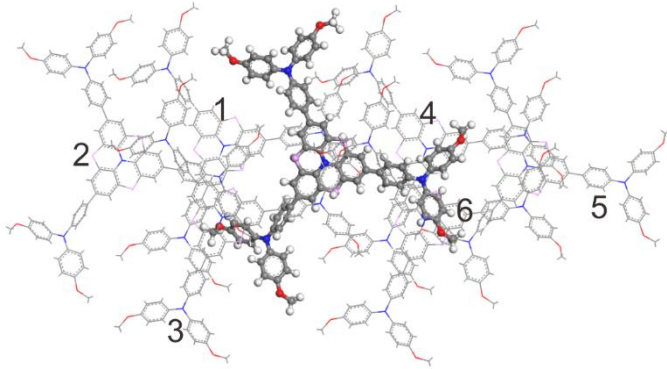
OMeTPA-P					
					
pathway	V_{DA}	k_h	r	μ_h	μ
1	6.47×10^{-5}	4.64×10^7	1.04×10^{-7}	9.71×10^{-6}	1.11×10^{-1}
2	-5.74×10^{-4}	3.64×10^{11}	2.03×10^{-7}	2.87×10^{-3}	
3	9.06×10^{-3}	9.07×10^{11}	1.36×10^{-7}	3.22×10^{-1}	
4	6.41×10^{-5}	4.55×10^7	1.04×10^{-7}	9.52×10^{-6}	
5	-5.73×10^{-4}	3.63×10^{11}	2.03×10^{-7}	2.86×10^{-3}	
6	9.07×10^{-3}	9.11×10^{11}	1.40×10^{-7}	3.44×10^{-1}	

Table S10 The transfer integrals V_{DA} (eV), hole-hopping rate k_h (s^{-1}), centroid-to-centroid distances r (cm), the hole mobility μ_h ($cm^2 v^{-1} s^{-1}$) for main hopping pathways selected and the total hole mobility μ ($cm^2 v^{-1} s^{-1}$) based on the predicted crystalline structures of **OMeTPA-As**.

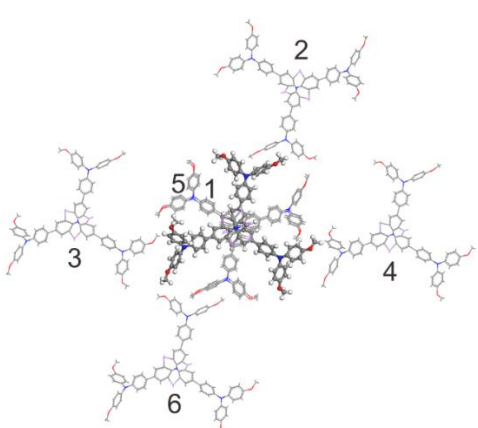
OMeTPA-As					
					
pathway	V_{DA}	k_h	r	μ_h	μ
1	-3.64×10^{-2}	9.96×10^{12}	3.52×10^{-8}	2.37×10^{-1}	7.91×10^{-2}
2	-2.91×10^{-4}	6.40×10^8	6.98×10^{-8}	6.00×10^{-5}	
3	4.67×10^{-7}	1.64×10^3	2.58×10^{-7}	2.11×10^{-9}	
4	1.41×10^{-7}	1.50×10^2	2.64×10^{-7}	2.01×10^{-10}	
5	-3.64×10^{-2}	9.97×10^{12}	3.52×10^{-8}	2.37×10^{-1}	
6	-2.91×10^{-4}	6.36×10^8	6.98×10^{-8}	5.96×10^{-5}	

Table S11 The transfer integrals V_{DA} (eV), hole-hopping rate k_h (s^{-1}), centroid-to-centroid distances r (cm), the hole mobility μ_h ($cm^2 v^{-1} s^{-1}$) for main hopping pathways selected and the total hole mobility μ ($cm^2 v^{-1} s^{-1}$) based on the predicted crystalline structures of **OMeTPA-O**.

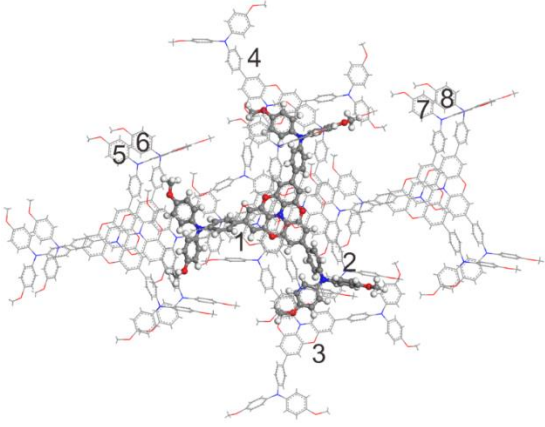
OMeTPA-O					
					
pathway	V_{DA}	k_h	r	μ_h	μ
1	5.05×10^{-5}	3.84×10^6	7.41×10^{-8}	4.05×10^{-7}	9.93×10^{-3}
2	5.07×10^{-5}	3.86×10^6	7.41×10^{-8}	4.08×10^{-7}	
3	7.55×10^{-3}	8.56×10^{10}	1.35×10^{-7}	2.99×10^{-2}	
4	7.54×10^{-3}	8.54×10^{10}	1.35×10^{-7}	2.98×10^{-2}	
5	-2.65×10^{-4}	1.06×10^8	2.01×10^{-7}	8.21×10^{-5}	
6	-2.51×10^{-4}	9.47×10^7	1.76×10^{-7}	5.64×10^{-5}	
7	-2.51×10^{-4}	9.45×10^7	1.76×10^{-7}	5.63×10^{-5}	
8	-2.65×10^{-4}	1.06×10^8	2.01×10^{-7}	8.22×10^{-5}	

Table S12 The transfer integrals V_{DA} (eV), hole-hopping rate k_h (s^{-1}), centroid-to-centroid distances r (cm), the hole mobility μ_h ($cm^2 v^{-1} s^{-1}$) for main hopping pathways selected and the total hole mobility μ ($cm^2 v^{-1} s^{-1}$) based on the predicted crystalline structures of **OMeTPA-S**.

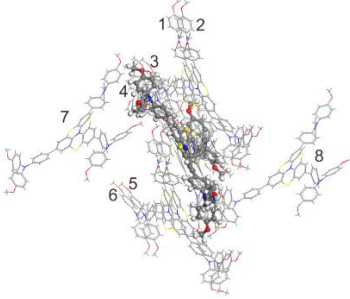
OMeTPA-S					
					
pathway	V_{DA}	k_h	r	μ_h	μ
1	2.92×10^{-3}	1.32×10^{11}	1.05×10^{-7}	2.81×10^{-2}	2.30×10^{-1}
2	2.92×10^{-3}	1.32×10^{11}	1.07×10^{-7}	2.88×10^{-2}	
3	-1.36×10^{-2}	2.86×10^{12}	1.15×10^{-7}	7.21×10^{-1}	
4	-1.36×10^{-2}	2.86×10^{12}	1.15×10^{-7}	7.21×10^{-1}	
5	-1.02×10^{-4}	1.62×10^8	1.17×10^{-7}	4.28×10^{-5}	
6	-1.05×10^{-4}	1.71×10^8	1.17×10^{-7}	4.51×10^{-5}	
7	1.05×10^{-4}	1.69×10^8	1.63×10^{-7}	8.68×10^{-5}	
8	1.05×10^{-4}	1.69×10^8	1.63×10^{-7}	8.69×10^{-5}	

Table S13 The transfer integrals V_{DA} (eV), hole-hopping rate k_h (s^{-1}), centroid-to-centroid distances r (cm), the hole mobility μ_h ($cm^2 v^{-1} s^{-1}$) for main hopping pathways selected and the total hole mobility μ ($cm^2 v^{-1} s^{-1}$) based on the predicted crystalline structures of **OMeTPA-Se**.

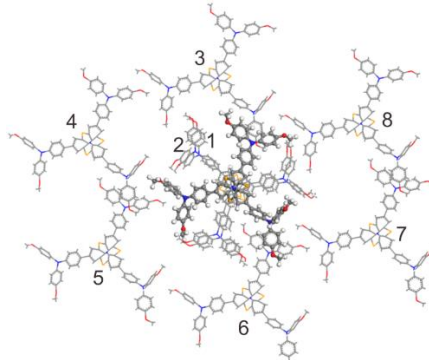
OMeTPA-Se					
					
pathway	V_{DA}	k_h	r	μ_h	μ
1	-7.85×10^{-2}	7.10×10^{13}	3.62×10^{-8}	1.78×10^0	5.94×10^{-1}
2	-7.84×10^{-2}	7.09×10^{13}	3.62×10^{-8}	1.78×10^0	
3	3.8×10^{-5}	2.67×10^2	1.93×10^{-7}	1.90×10^{-10}	
4	-1.52×10^{-7}	7.71×10^5	2.61×10^{-7}	1.01×10^{-6}	
5	8.18×10^{-6}	1.59×10^7	2.46×10^{-7}	1.85×10^{-5}	
6	3.72×10^{-5}	1.59×10^7	1.93×10^{-7}	1.14×10^{-5}	
7	-1.48×10^{-7}	2.52×10^2	2.61×10^{-7}	3.32×10^{-10}	
8	8.26×10^{-6}	7.86×10^5	2.46×10^{-7}	9.15×10^{-7}	

Table S14 The combination modes and surface adsorption energy (eV) of central core and perovskite surface (001 face).

Molecule	the surface adsorption energy (eV)		The most stable combination mode
	Pb-N controlled	Pb-X controlled	
OMeTPA-TPA	-0.69	-0.32	Pb-N controlled
OMeTPA-B	-0.78	-1.26	Pb-X controlled
OMeTPA-C	-1.19	-1.12	Pb-N controlled
OMeTPA-Si	-0.81	-0.57	Pb-N controlled
OMeTPA-Ge	-1.23	-0.89	Pb-N controlled
OMeTPA-N	-1.73	-1.19	Pb-N controlled
OMeTPA-P	-0.81	-0.53	Pb-N controlled
OMeTPA-As	-0.86	-0.61	Pb-N controlled
OMeTPA-O	-1.01	-1.17	Pb-X controlled
OMeTPA-S	-1.25	-1.82	Pb-X controlled
OMeTPA-Se	-1.26	-1.85	Pb-X controlled

Table S15 The optimized structures of Pb-N and Pb-X models of central core and perovskite surface (001 face).

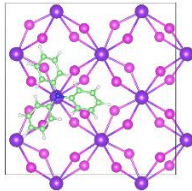
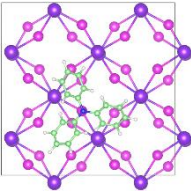
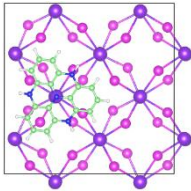
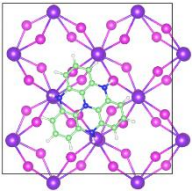
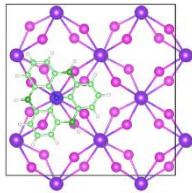
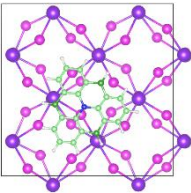
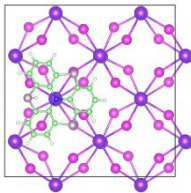
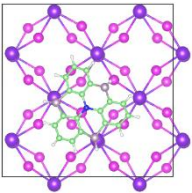
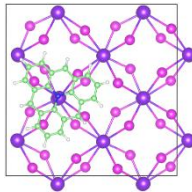
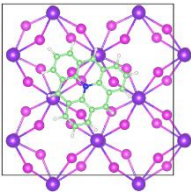
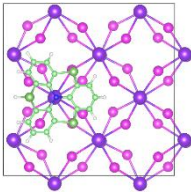
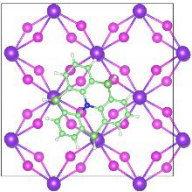
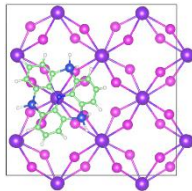
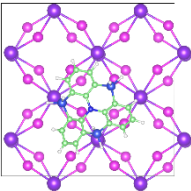
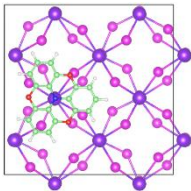
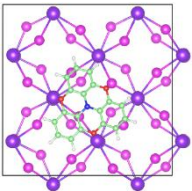
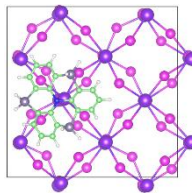
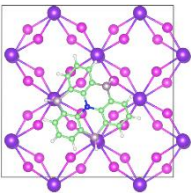
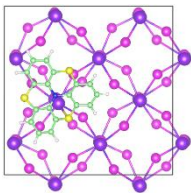
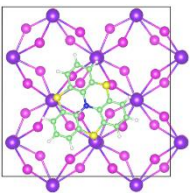
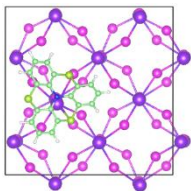
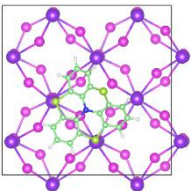
	Pb-N controlled	Pb-X controlled		Pb-N controlled	Pb-X controlled
R-TPA			R-N		
R-B			R-P		
R-C			R-As		
R-Si			R-O		
R-Ge			R-S		
			R-Se		

Table S16 The Pb-N (Pb-X) bond lengths (Å) of the most stable combination mode of central core and perovskite surface (Corresponding to the structure in **Figure S5**).

Molecule	The most stable combination mode	Figure S5		
		Pb-N bond lengths (Å)	Pb-X1 bond lengths (Å)	Pb-X2 bond lengths (Å)
OMeTPA-TPA	Pb-N controlled	4.70	/	/
OMeTPA-B	Pb-X controlled	/	3.24	3.35
OMeTPA-C	Pb-N controlled	2.90	/	/
OMeTPA-Si	Pb-N controlled	4.63	/	/
OMeTPA-Ge	Pb-N controlled	3.47	/	/
OMeTPA-N	Pb-N controlled	4.03	/	/
OMeTPA-P	Pb-N controlled	4.76	/	/
OMeTPA-As	Pb-N controlled	4.64	/	/
OMeTPA-O	Pb-X controlled	/	3.09	3.12
OMeTPA-S	Pb-X controlled	/	3.11	3.05
OMeTPA-Se	Pb-X controlled	/	3.11	3.11

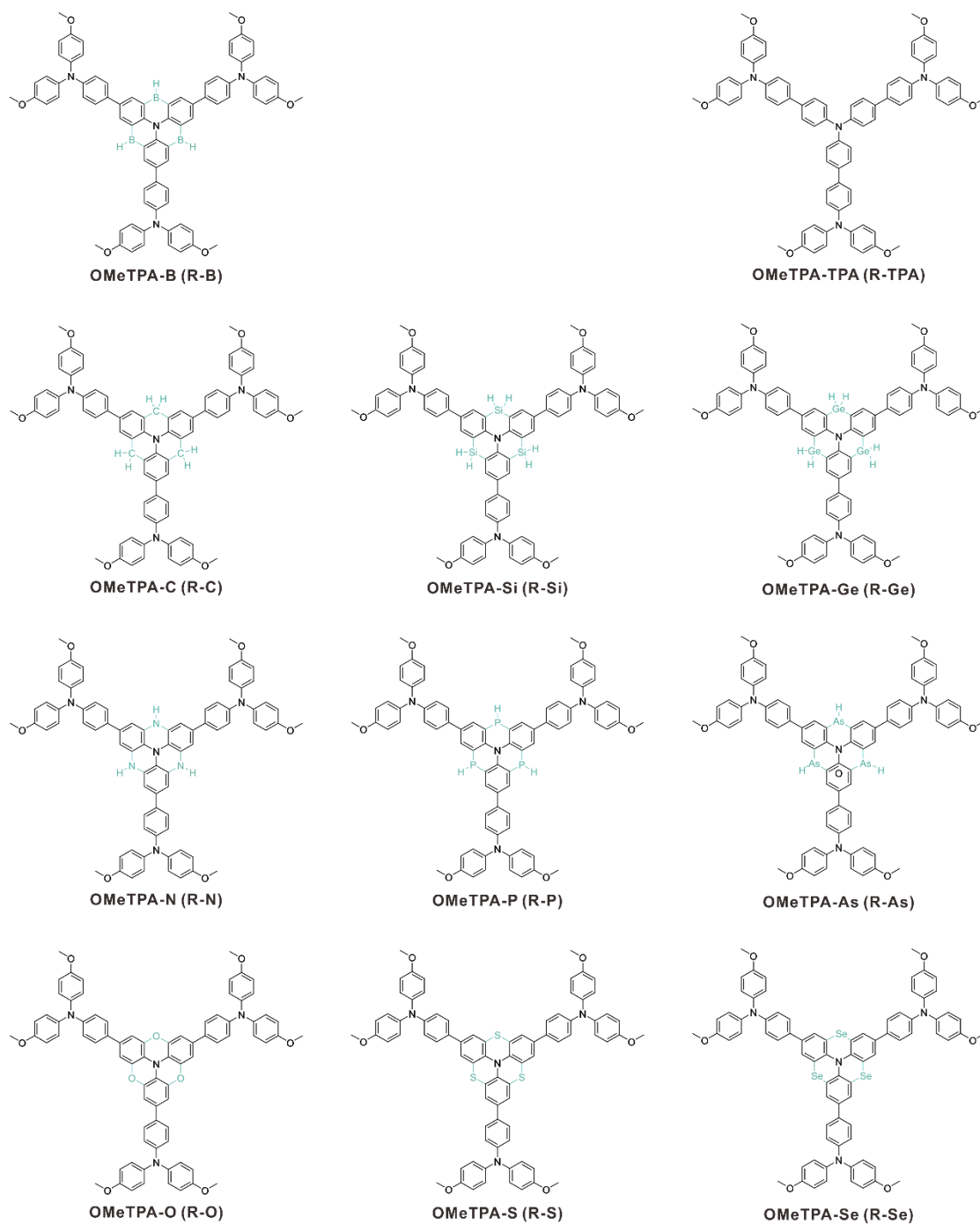


Figure S1 The chemical structures and full names of the study molecules.

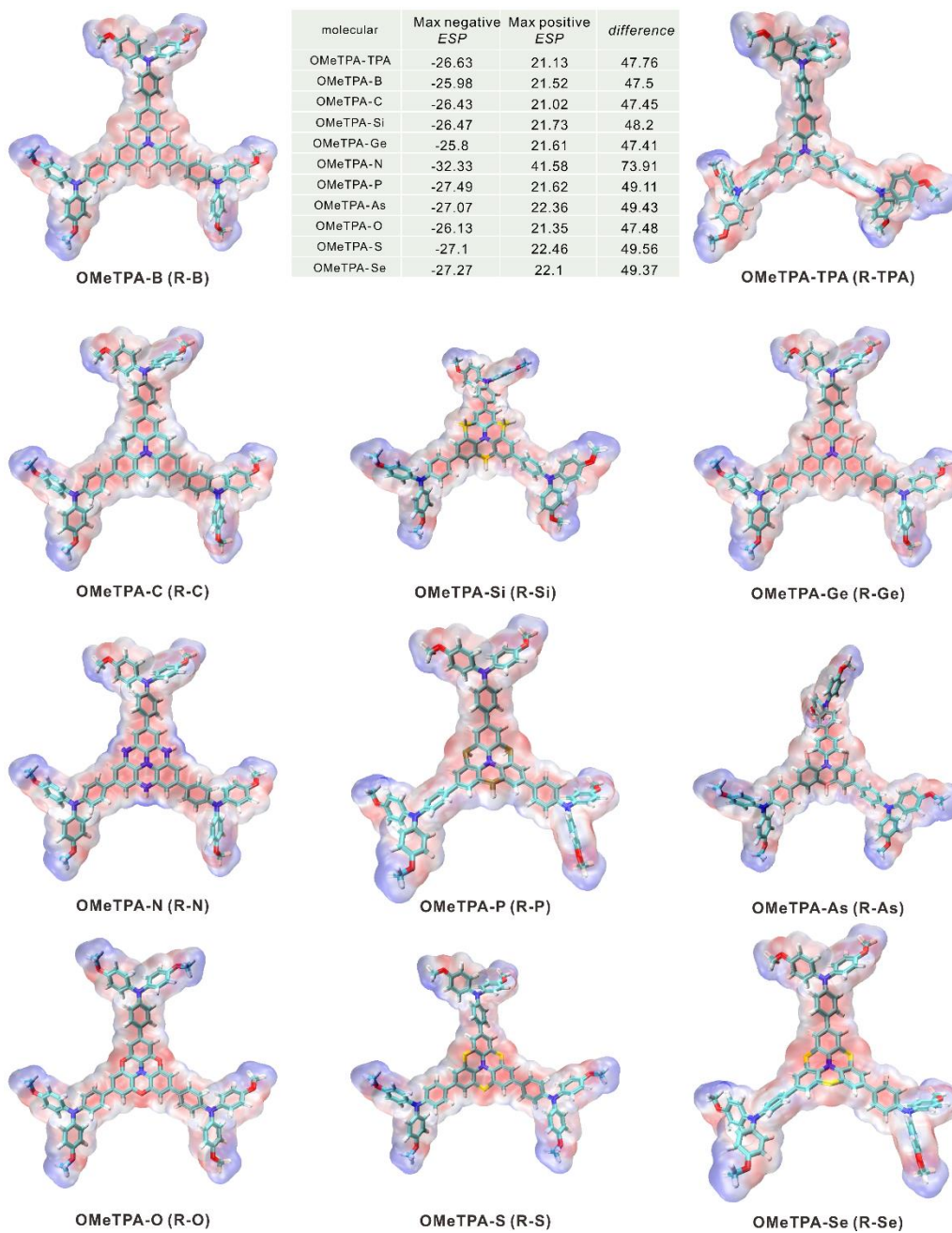


Figure S2 Molecular electrostatic potentials (*ESP*) of **R-TPA** and **R-X**, along with the Max positive *ESP*, Max negative *ESP*, and the difference between positive and negative *ESP* of the investigated molecules, units are expressed in kcal mol⁻¹.

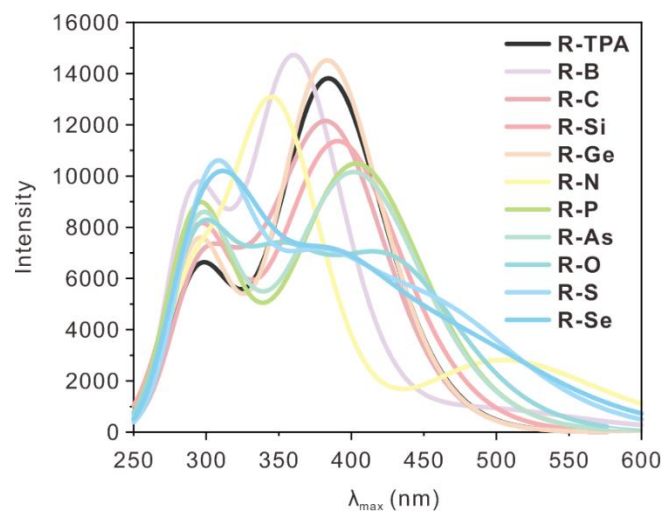


Figure S3 Calculated absorption spectra of the studied molecules.

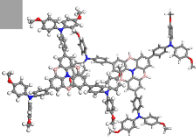
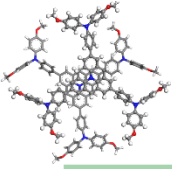
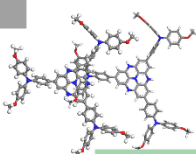
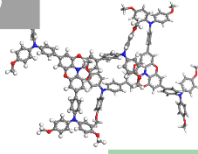
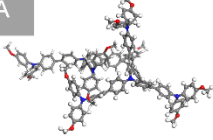
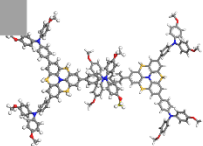
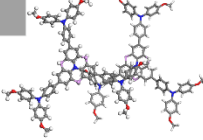
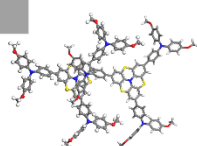
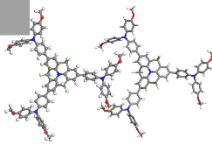
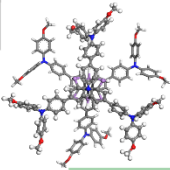
B		C		N		O	
	0.16 1.38×10^{-7} 1.03×10^{-3} 0.001		0.13 4.17×10^{-8} -1.31×10^{-2} 0.029		0.42 1.22×10^{-7} -1.45×10^{-3} 0.00009		0.31 1.35×10^{-7} 7.55×10^{-3} 0.010
TPA		Si		P		S	
	0.12 1.07×10^{-7} -1.46×10^{-3} 0.002		0.15 2.02×10^{-7} 9.40×10^{-3} 0.127		0.14 1.40×10^{-7} 9.07×10^{-3} 0.111		0.12 1.15×10^{-7} -1.36×10^{-2} 0.230
reorganization energy (λ, eV)				Ge		As	
centroid distances (r, cm)					0.21 2.08×10^{-7} -1.87×10^{-3} 0.004		0.17 3.52×10^{-8} -3.64×10^{-2} 0.079
transfer integrals (V, eV)							0.14 3.62×10^{-8} -7.85×10^{-2} 0.594
hole mobility (μ_h, $\text{cm}^2 \text{v}^{-1} \text{s}^{-1}$)							

Figure S4 The main neighboring hole-hopping pathways selected based on the predicted crystal structures for all molecules, along with the reorganization energy λ (eV, green one), centroid-to-centroid distances r (cm, blue one), transfer integrals V (eV, orange one) and the hole mobility μ_h ($\text{cm}^2 \text{v}^{-1} \text{s}^{-1}$, purple one) for main hopping pathways selected based on the predicted crystalline structures.

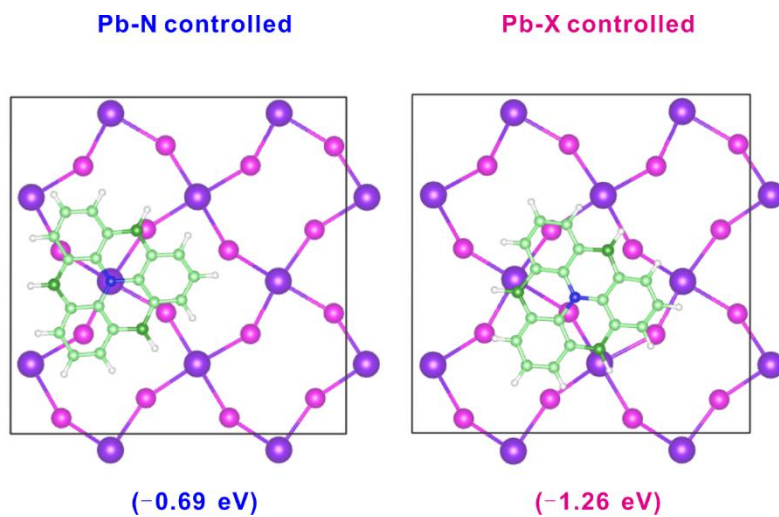


Figure S5 The combination mode of central core and perovskite surface (001 face)

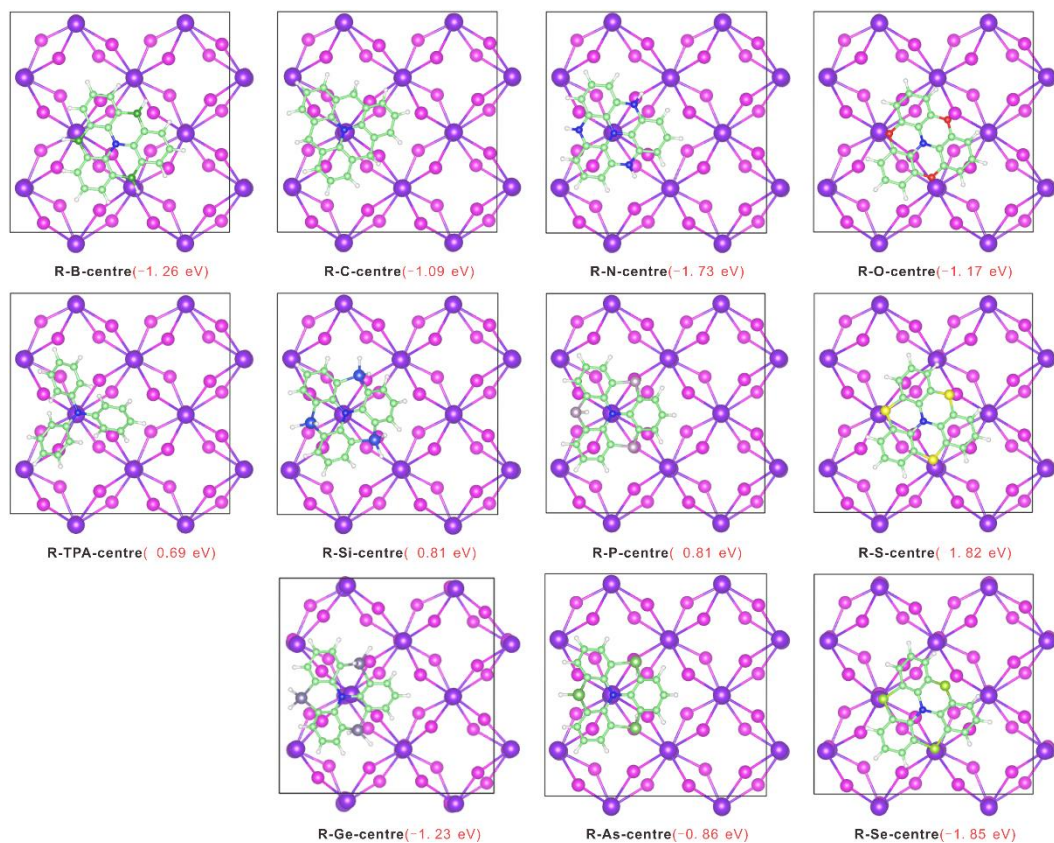


Figure S6 The most stable combination mode of central core and perovskite surface (001 face)

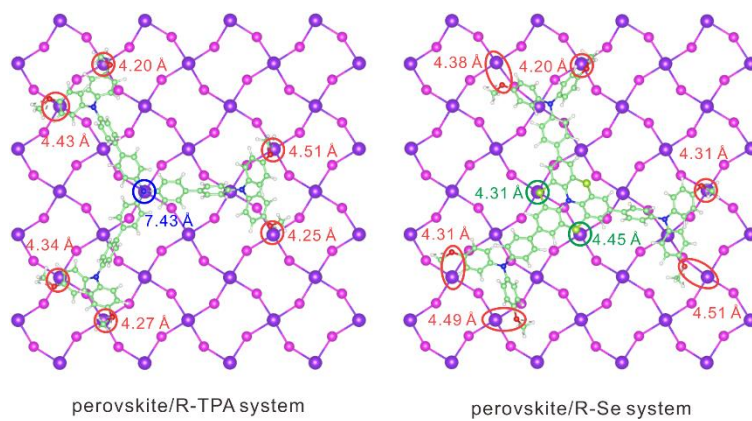


Figure S7 The key bond lengths in perovskite/**R-TPA** and perovskite/**R-Se** systems.

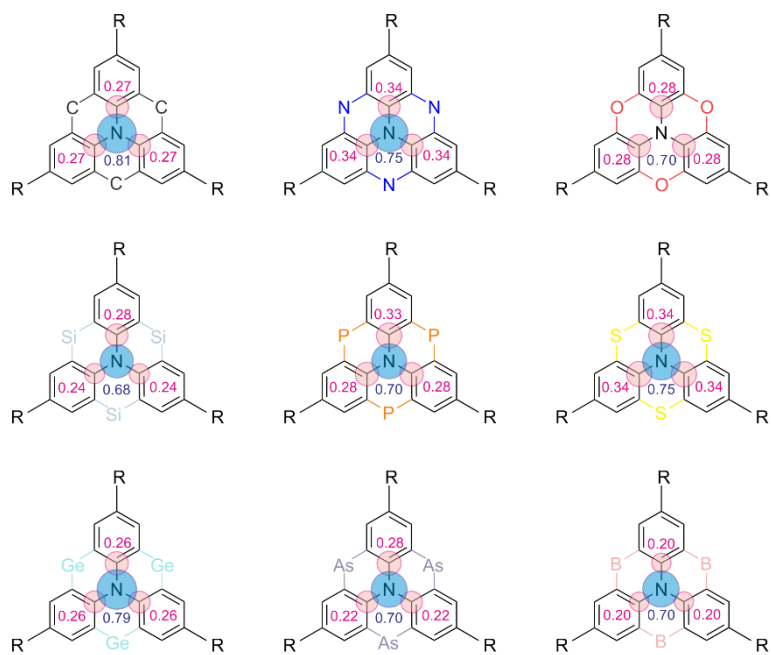


Figure S8 The distribution of partial atomic charges for **R-B**, **R-C**, **R-Si**, **R-Ge**, **R-N**, **R-P**, **R-As**, **R-O**, and **R-S**, where blue represents negative charge and pink represents positive charge.

References

1. J. Cornil, V. Lemaire, J.-P. Calbert and J.-L. Brédas, *Adv. Mater.*, 2002, **14**, 726-729.
2. R. A. Marcus, *Angew. Chem. Int. Ed.*, 1993, **32**, 1111 - 1222.
3. G. Nan, L. Wang, X. Yang, Z. Shuai and Y. Zhao, *J. Chem. Phys.*, 2009, **130**, 024704.
4. W. Linjun, N. Guangjun, Y. Xiaodi, P. Qian, L. Qikai and S. Zhigang, *Chem. Soc. Rev.*, 2010, **39**, 423-434.
5. S. Grimme, J. Antony, S. Ehrlich and H. Krieg, *J. Chem. Phys.*, 2010, **132**, 154104.